BBA - Proteins and Proteomics 1868 (2020) 140481

Contents lists available at ScienceDirect

BBA - Proteins and Proteomics

journal homepage: www.elsevier.com/locate/bbapap

Analysis of Hashimoto's thyroiditis on fine needle aspiration samples by MALDI-Imaging

Giulia Capitoli[a,1], Isabella Piga[f,1], Francesca Clerici[f,1], Virginia Brambilla[b], Allia Mahajneh[f], Davide Leni[c], Mattia Garancini[d], Angela Ida Pincelli[e], Vincenzo L'Imperio[b], Stefania Galimberti[a], Fulvio Magni[f,*], Fabio Pagni[b,*]

[a] Bicocca Bioinformatics Biostatistics and Bioimaging B4 Center, School of Medicine and Surgery, University of Milano - Bicocca, Monza, Italy
[b] Pathology, Department of Medicine and Surgery, University of Milano-Bicocca, San Gerardo Hospital, ASST, Monza, Italy
[c] Department of radiology, San Gerardo Hospital, ASST, Monza, Italy
[d] Department of Surgery, San Gerardo Hospital, ASST, Monza, Italy
[e] Department of Endocrinology, San Gerardo Hospital, ASST, Monza, Italy
[f] Proteomics and Metabolomics, School of Medicine and Surgery, University of Milano-Bicocca, Vedano al Lambro, Italy

ARTICLE INFO

Keywords:
MALDI-TOF
Mass spectrometry-imaging
Hashimoto thyroiditis
Proteomics

ABSTRACT

Matrix-Assisted Laser Desorption/Ionization (MALDI)-Mass Spectrometry imaging (MSI) has been applied in various diseases aimed to biomarkers discovery. In this study diagnosis and prognosis of Hashimoto Thyroiditis (HT) in cytopathology by MALDI-MSI has been investigated. Specimens from a routine series of subjects who underwent UltraSound-guided thyroid Fine Needle Aspirations (FNAs) were used. The molecular classifier trained in a previous study was modified to include HT as a separate entity in the group of benign lesions, in the diagnostic proteomic triage of thyroid nodules. The statistical analysis confirmed the existence of signals that HT shares with hyperplastic lesions and others that are specific and characterize this subgroup. Statistically relevant HT-related peaks were included in the model. Then, the discriminatory capability of the classifier was tested in a second validation phase, showing a good agreement with cytological diagnoses. The possibility to overlap the molecular signatures of both the lymphocytes and epithelial cells components (ROIs or pixel-by-pixel analysis) confirmed the composite proteomic background of HT. These results open the way to their possible translation as alternative serum biomarkers of this autoimmune condition.

1. Introduction

Matrix-Assisted Laser Desorption/Ionization (MALDI)-Mass Spectrometry imaging (MSI) has been applied in normal and pathological tissues aimed to biomarkers discovery [1–3]. MALDI-MSIis a special proteomic approach that allows the localization and the expression analysis of different types of molecules within the tissue, without the need of any labelling or extraction process. Specimens (fresh frozen samples, formalin-fixed paraffin-embedded (FFPE) whole sections or tissue microarray) can be analysed directly by MALDI-TOF avoiding the preliminary step of extraction of the molecules of interest that hinder the information about localization [4]. For this reason, the popularity of MALDI-MSI increased in last years and has been extensively used in different fields with promising results [5]. In particular, pivotal experiments tested MALDI-MSI to detect differences in the protein signatures of thyroid lesions [3,6]. More intriguing is the possibility to investigate specimens collected by thyroid fine-needle aspirates (FNAs) [1]. The recent technical improvements of the laser used for MALDI analysis, enable the detection of cell subpopulations based on their different protein profiles, even within regions that are indistinguishable at the microscopic level [5,7]. Hashimoto thyroiditis (HT) is an autoimmune disease characterized by a lymphocytic infiltrate intermingled with the epithelial (follicular) cells normally resident in the thyroid parenchyma [8]. Patients with HT often undergo thyroid FNA due to the occurrence of suspicious nodules; moreover, serial ultrasound (US) examinations are performed considering the possible pathogenetic relationship between HT and cancer [9]. To date, HT management is based on a combination of serological, US and cytological tests [10–12]. Based on the previous findings, HT belongs to the group of benign thyroid lesions being the second most frequent

* Corresponding authors at: Department of Medicine and Surgery, University Milan – Bicocca, Monza; Italy.
E-mail addresses: fulvio.magni@unimib.it (F. Magni), fabio.pagni@unimib.it (F. Pagni).
[1] Equally contributing authors

https://doi.org/10.1016/j.bbapap.2020.140481
Received 29 February 2020; Received in revised form 4 June 2020; Accepted 27 June 2020
Available online 06 July 2020

Table 1
Clinical and hystological information for the training and validation cohorts.

Hp: Hyperplastic; HT: Hashimoto Thyroiditis; HR: Hormone Replacement; PTC: Papillary Thyroid Carcinoma; TPO-Ab: Thyroid Peroxidase antibody; Tg-Ab: Thyroglobulin antibodies.

Training									
	Patient ID	Age (years)	Sex	Nodule Size (cm)	Therapy	Type	Interval	Dose	
Hp	262	81	F	3	No				
	268	82	F	1.5	No				
	275	55	F	2.5	No				
	302	64	F	1.5	No				
	308	33	F	1	No				
	384	72	F	2	HR	Tapazole	90 days	30 mg	
	565	70	M	2.5	No				
	1046	57	F	1.8	No				
	381	69	F	1.2	HR	L-Thyroxine	8 years	50 mcg	
	Patient ID	Age (years)	Sex	Nodule Size (cm)	Therapy	Type	Interval	Dose	
PTC	213	49	F	1.4	HR	L-Thyroxine	1 month	125 mcg	
	250	88	F	3	HR	L-Thyroxine	1 year	100 mcg	
	442	41	F	2.5	HR	Liothyronine	1 month	10 mcg	
	992	47	F	1	No				
	995	62	F	5	No				
	1012	70	M	2	No				
	1076	39	F	1.3	No				
	1187	24	F	1.7	No				
	1126	55	M	2	No				

	Patient ID	Age (years)	Sex	Nodule Size (cm)	Interval HT diagnosis-FNA (months)	Therapy	Type	Interval	Dose	TPO-Ab/ Tg-Ab
HT	598	57	F	2.1	96	No				+
	647	39	F	1.9	36	No				+
	922	31	M	1.6	3	No				+
	1047	63	F	1.1	1	No				-
	1083	50	F	1	1	No				+
	1144	67	F	1.6	3	No				+
	1145	42	F	1	1	No				-
	1208	63	M	1.7	12	No				+
	1074	80	F	2	1	No				-

Validation											
CYTOLOGICAL DIAGNOSIS		Patient ID	Age (years)	Sex	Nodule Size (cm)	Interval HT diagnosis-FNA (months)	Therapy	Type	Interval	Dose	TPO-Ab/Tg-Ab
THY 2	Hp	1123	36	F	2.5		HR	L-Thyroxine	5 years	50 mcg	
THY 2	Hp	1156	53	F	1.1		No				
THY 2	Hp	1123	36	F	2.5		HR	L-Thyroxine	5 years	50 mcg	
THY 2	Hp	1156	53	F	1.1		No				
THY 2	Hp in thyroiditis	278	63	F	4	204	No				+
THY 2	HT	316	71	F	3.5	1	HR	L-Thyroxine	17 years	75 mcg	+
THY 2	HT	520	65	F	0.8	228	HR	L-Thyroxine	6 months	75 mcg	+
THY 2	HT	525	51	F	1.7	84	HR	L-Thyroxine	7 years	100 mcg	+
THY 2	HT	1075	46	F	2.5	7	No				+
THY 2	HT	1081	79	F	3.5	1	No				-
THY 2	HT	1122	77	F	1	1	No				-
THY 2	HT	1234	53	F	1	1	No				-
THY 3A	HT	1082	50	F	3.5	1	No				-
THY 4	PTC	1202	37	M	2		No				
THY 5	PTC	1084	61	M	1.1		No				
THY 5	PTC	1149	31	F	1.7		No				
THY 5	PTC	1188	24	F	2		No				
THY 5	PTC in thyroiditis	11171	54	F	1.5	1	No				-

entity with hyperplastic nodules (Hp). Hps are follicular proliferations with occasional metaplastic features like oncocytic changes; these second findings are typical of HT near to the florid lymphocitic component. Basically, nuclear alterations typical of papillary thyroid carcinoma (PTCs) are absent or only barely outlined. In the current study, we have investigated the possible application of MALDI-MSI in cytopathology to help clinicians for a better diagnosis and prognosis of HT.

2. Material and methods

A prospective consecutive series of 1355 US-guided FNAs performed on subjects enrolled in an AIRC-granted clinical study aimed to find new diagnostic markers for thyroid lesions, were used for the present study.

A subset of this large cohort of patients was selected using as inclusion criteria the serological positivity to anti-thyroperoxidase antibodies (TPO-Ab, > 34 IU/mL) and/or anti-thyroglobulin Ab (Tg-Ab > 115 IU/mL) or a US diagnostic pseudonodular appearance at imaging. In particular $n = 6$ patients in the training set and $n = 5$ patients in the validation set (Table 1) were positive to TPO-Ab and/or Tg-Ab; while the pseudonodular appearance is present in $n = 3$ patients in the training set and $n = 2$ in the validation set. Moreover 2 patients with an histological diagnosis of spread lymphocitic thyroiditis on the surgical specimens were enrolled (case ID 1082 and 11171). A cohort of 27 patients (9 Hp, 9 PTC and 9 HT) were used for the training phase. Further 16 patients (3 Hp, 8 HT and 5 PTCs) were used to validate the classifier. The average time within the first HT clinical suspicion and FNA was available (mean = 35.95, range:1–228 months). Data regarding patients' therapy (type of drug, posology and timing) were collected and summarized with the relevant clinical–pathological characteristics for all the cases in the study in Table 1. The study was approved by the ASST Monza Ethical Board (Associazione Italiana Ricerca sul Cancro-AIRC-MFAG 2016 Id. 18445, HSG Ethical Board Committee approval October 2016, 27/10/2016). Appropriate informed consent was obtained from all patients included in the study.

2.1. Pathology

US-guided FNAs were performed using a 25-gauge needle at the Department of Radiology, San Gerardo Hospital, Monza, Italy. One or two passes per nodule were executed and needle washing from every pass was sent for proteomics MALDI-MSI analysis [13]. Pathologists evaluated the corresponding Pap-stained smears for traditional morphological diagnosis certifying the existence of diagnostic criteria of HT (*e.g.* the presence of a diffuse lymphocytic infiltrate, presence of germinal centers and oncocytic changes of epithelial cells).

2.2. In Situ proteomics: MALDI-MSI

Needle washing from thyroid FNAs were collected into a CytoLyt solution (20% buffered methanol-based solution, ThinPrep™ 2000 system, CYTYC Corporation, Hologic) and samples were prepared with a previously optimized sample preparation method able to remove the interference of haemoglobin, to preserve up to 14 days the samples and to provide reproducible results and finally transferred as a cytospin spot onto ITO glass slides [13,14]. Then, all slides were washed with increased concentration of ethanol (70%, 90%, and 95%) for 30 s each, dried under vacuum for 15 min, and stored at −80 °C until the day of the analysis (mean 24–48 h after the time of biopsy). Before MALDI-MSI analysis, cytological specimens were equilibrated to room temperature, dried under vacuum for 30 min, and the MALDI-matrix sinapinic acid (10 mg/mL in 60:40 acetonitrile:water w/0.2% trifluoroacetic acid) was uniformly deposited, with an optimized method, using the iMatrixSpray (Tardo GmbH, Subingen, Switzerland) automated spraying system. MALDI-TOF-MSI was performed using an ultrafleXtreme MALDI-TOF/TOF (Bruker Daltonik GmbH, Bremen, Germany) in positive-ion linear mode, using 300 laser shots per spot, with a laser focus setting of 3 medium (diameter of 50 μm) and a pixel size of 50 × 50 μm. Protein Calibration Standard I (Bruker Daltonics, Billerica, MA, USA), that contained a mixture of standard proteins within the mass range of 5,730 to 16,950 Da, was used for external calibration (mass accuracy ± 30 ppm). Spectra were recorded within the m/z 3,000–20,000 range. Data acquisition and visualization were performed using the Bruker software packages (flexControl 3.4, flexImaging 5.0). After the analysis, the MALDI matrix was removed with 70% EtOH and the slides were stained with haematoxylin and eosin (H&E), digitally scanned using a ScanScope CS digital scanner (Aperio, Park Center Dr., Vista, CA, USA), and images were coregistered to the MSI datasets in flexImaging for the integration of proteomic and morphological data. Regions of interest (ROIs) with pathological areas containing both thyrocytes and lymphocytes were comprehensively annotated.

2.3. Statistical analysis

The statistical analysis on proteomic data was performed on ROIs in the training phase, while for each patient in the validation set, three different approaches were tested: the average spectra generated from the MALDI-MSI analysis, the spectra from each ROI selected by the pathologist, and all the single spectra of the imzML MALDI-MSI analysis (pixel-by-pixel). The spectra were processed by performing baseline subtraction (median method), smoothing (moving average method, half window width 2.5), normalization (total ion current, TIC), peak alignment, and peak picking (S/N ≥ 6). The open-source software mMass v.5.5 (http://www.mmass.org) was used to confirm mass spectra alignment. Only peaks with an absolute intensity greater or equal than 0.0003, after TIC normalization, were retained. Intra- and inter-patient filters were applied on the detected features in the training set: (i) only the features (m/z) detected in at least 25% of the ROIs within the same patient were considered and (ii) the features (m/z) that were common to at least 25% of the Hps 25% of the PTCs and to the 25% of HTs were included in the model. For the groups in the training set a multinomial regression with a Lasso regularization method was performed. To select the Lasso penalizing parameter, and to assess the predictive accuracy within the training set, cross-validation was performed. The validation was done in blind from the patient's histological diagnosis and considering only the features selected by the Lasso model to quantify the probability to be malignant, hyperplastic or HT. For each pixel the probability to belong in the three classes (Hp, HT and PTC) were calculated. The highest of the three indices obtained from each single spectrum was used to classify the corresponding pixel. Quartiles, ranges, mean, and standard deviation (sd) were calculated to provide an overview of the data for the whole sample in the pixel-by-pixel classification. To further assess spectra similarities of the training phase, Principal Component Analysis (PCA) were also performed. Before the PCA analysis, data were scaled and centered. Data preprocessing (MALDIquant package) and statistical analyses (glmnet and prcomp package) were performed using the open-source R software v.3.6.0.

3. Results

The capability of MALDI-MSI to generate molecular signatures and distinguish HT from Hp nodules and from PTC was investigated. The PCA clearly showed an evident difference between PTC and Hp and an overlap between HT and Hp (Fig. 1). This results suggested the existence of signals that HT shares with goiter. However, specific molecular findings generated a HT-linked profile. This could be expected because Hp and HT share common epithelial cells, differing mainly for the lymphocytic component of the inflammatory background. Comparing HT and classic goiter that was characterized in our previous study [3], the existence of an additional component could have relevant implications in the training phase of the proteomic classifier. These

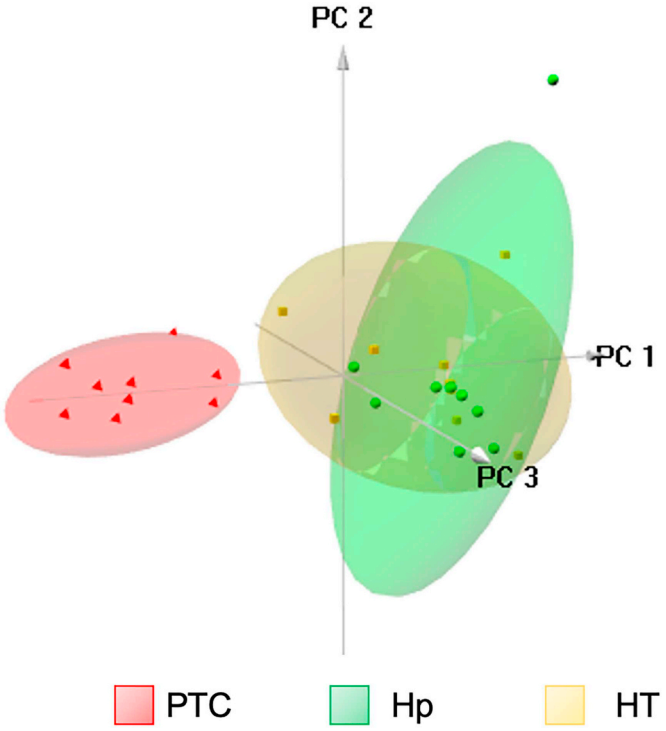

Fig. 1. Principal component analysis of n = 9 papillary carcinoma (PTC, red), *n* = 9 hyperplastic (Hp, green) and n = 9 Hashimoto thyroiditis (HT, yellow) patients using the overall average spectra of each sample.

results confirmed that HT belongs to the group of benign lesions, basically, even with own specific molecular trait (Fig. 1). Therefore, the model was learnt to recognize as benign this particular entity. Equivalent groups of ROIs were generated (5 groups of ROIs for cluster of benign thyrocytes, 4 ROIs for cluster of malignant thyrocytes and 5 groups of ROIs for cluster of epithelial and lymphocytes in HT). Therefore, 45 mean spectra were generated for Hp and HT and 36 for the malignant lesions to be used for the statistical analysis of the training data. Typical example of results from the pixel-by-pixel evaluation are reported in Fig. 2, in which 5 patients of the training phase were reported highlighting the different types of molecules within the tissue. The green area of P_302 clearly shows the homogenous benign profile of Hp while the diffuse red area in the P_992 specimens strongly suggests PTC. The yellow area for P_1144, P_1047 and P_1083 shows undeniable evidence of HT in different percentage (bold numbers) of benign thyrocytes and lymphocytes background, with different profile from Hp and PTC. Moreover, the possibility to distinguish lymphocytes from epithelial cells based on specific signals is elighten in Fig. 3. In particular 2 signals of the average protein profile were able to distinguish where lymphocytes (pink) and epithelial (green) cells were localised overlapping with H&E (Fig. 3c and d). Then, the frequency of inflammatory background based on pixel-by-pixel elaboration of the MSI data was evaluated (Fig. 2). Results were found in rather good agreement with the percentage of epithelial and lymphocytes cells observed in the cytological evaluation by pathologists (Table 2). The previously described model, once updated, was used to evaluate the probability of the three different types of lesions in the cohort of patients included of the validation phase. Statistical data elaboration clearly showed a good agreement between cytological diagnosis and MSI with few exceptions (Table 2, Supplementary Table 1–2). The model correctly classified all the benign lesions (Hp) and for HT the different percentage of epithelial and inflammatory background (Table 2 and Supplementary Table 2). Two of these cases showed a good agreement between the cytological evaluation of the percentage of epithelial and lymphocytes cells and pixel-by-pixel classification (*e.g.* P_1081 showed 90% homogeneous lymphocytes composition and P_520 showed 50–50% mixture of epithelial and inflammatory background) (Supplementary Fig. 1A-B). Two HT patients (P_525 and P_1075) in addition to epithelial and lymphocytes showed some signals of alert (Supplementary Fig. 1G-H). Moreover, the model was able to detect a PTC profile (P_11171) without being deceived by the inflammatory background (Supplementary Fig. 1C and Supplementary Table 1–2). The average spectrum of the entire area of the P_1149 sample seems to misclassified the patient. However, the singles ROIs and, more important, the pixel-by-pixel classification shows an undateable malignancy (Supplementary Fig. 1F). Only patients P_1084 and the P_1188 were misclassified as benign instead of PTC, due to the paucity of the cells [3]. In fact, an enriched specimen of the same patient taken after surgery on thyroidectomy (*ex vivo* FNA) was correctly classified using both ROIs and pixel-by-pixel data (Supplementary Table 1–2 and Supplementary Fig. 1F). Interestingly, the model was able to correctly classified also “indeterminate” cases: P_1082 (THY3) and P_1202 (THY4) which were classified as benign and PTC respectively, in agreement with their histological diagnosis after total thyroidectomy (Supplementary Fig. 1D-E). These results are in accordance with those obtained in our previous experiments and support the hypothesis that MALDI-MSI could better enlighten the nature of the lesion because of its capability to preserve both the localization of the proteins and the tissue morphology which is lost with the classical extractive proteomics strategies [3]. Therefore, we could focus on the proteomic profiles of specific regions of interests (thyrocytes cell clusters or the inflammatory background) involved in thyroid nodule formation or in Hashimoto's thyroiditis disease occurrence. In the pixel-by-pixel statistical data elaboration, malignant and benign lesions associated with different grade of synchronous HT are easily diagnosed again (Supplementary Table 2 and Supplementary Fig. 1). The probability to be malignant in the training phase of Hp and HT observed in the 3rd quartile is very low (< 7.55%) while in PTC the malignancy probability is already above 21% in the 1st quartile (Supplementary Table 2). In the following validation phase, the classifier was working in blind to diagnostic judgement of cytological specimens, previously classified as HT at microscopy. Behind the correct classification an additional important advantage of the MALDI-MSI is its capability to differentiate the different cellular component as above described.

4. Discussion

HT is a chronic autoimmune disease of the thyroid; with the progressive introduction of thyroid function and autoantibodies testing its incidence increased, being today the most common endocrine disorder in well-developed countries [15,16]. The diagnosis is based on serological and US assessment [17,18]. However, both in the diagnostic phase and prognostic management, improvements may be reached by the introduction of more precise clinical tools. Thyroid sonography characteristically shows a diffusely heterogeneous parenchyma with reduced echogenicity, or multiple ill-defined small nodules (pseudonodules). Although the histological findings of a diffuse lymphocytic infiltration and pseudonodular oxyphilic metaplasia remain the gold standard, thyroidectomy is rarely performed. Despite the presence of clinically proven disease (hypothyroidism and pseudonodular atrofic US pattern), young patients often have lower titers or even negative circulating TPO-Ab. On the contrary, US thyroiditis-like patterns may be found in 20% of individuals without detectable antibodies [19]. The prevalence of elevated TPO-Ab and Tg-Ab antibodies in the general population is around 10%, but it increases with age and is more common in women [20]. However, the prevalence of spontaneous hypothyroidism in iodine-sufficient populations is much lower (~1–2%) [21]. Finally, the pathogenetic prognostic relationship between HT and cancer is debated too [22,23]. In the last years, targeted and untargeted proteomic have been widely employed on clinical specimens (*e.g.* plasma, urine, saliva, tissue, cytological samples) as powerful tools for

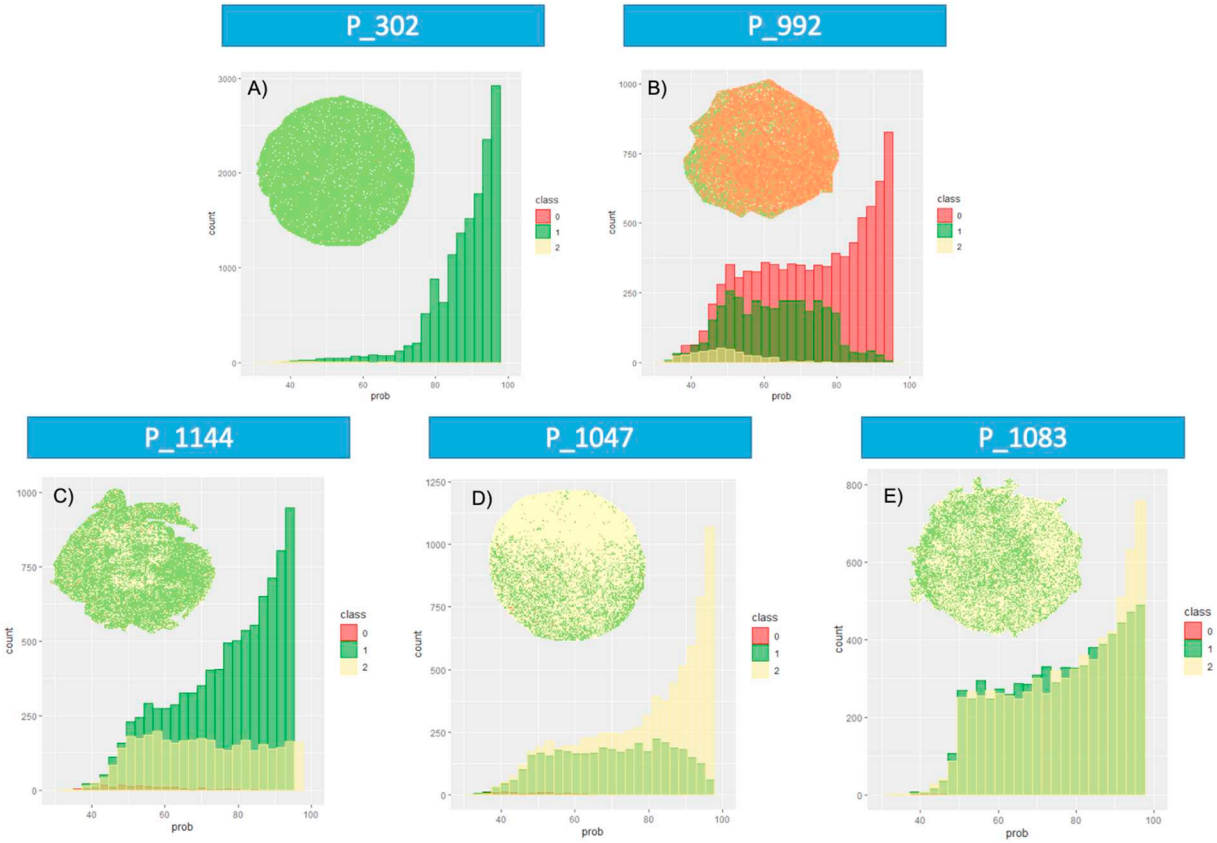

Fig. 2. Pixel-by-pixel classification of imzml analysis of six patients and their histogram of frequency: A) P_302 is a hyperplastic (Hp) patient; B) P_992 is a papillary thyroid carcinoma patient (PTC); C) P_1144 is a patient with a morphology of ~90% of epithelial cells and ~ 10% of lymphocytes cells; D) P_1047 is a patient with a morphology of ~90% of lymphocytes cells and ~ 10% of epithelial cells; E) P_1083 is a patient with a morphology of ~50% of epithelial cells and ~ 50% of lymphocytes cells. Class 0 (red) represent PTC spectra; class 1 (green) represent Hp spectra; class 2 (yellow) represent HT spectra.

biomarker discovery in many cancers such as kidney, breast, gastric and thyroid [3,24–26] but also autoimmune diseases [27–29]. However, these classical approaches are not applicable to this study in which specific protein profile for specific cell types present in the FNAs has to be obtained. The group of cytological specimens from HT are relevant to be investigated for the future application of MALDI-MSI and of its findings, both in FNAs but also for future translation to serum samples, in clinical settings. Previous studies, done using MALDI-QIT-TOF-MS/MS to evaluate the glycosylation profiles of autoAb, confirmed that TgAb may have a role in the pathogenesis of HT. IgG of HT patients

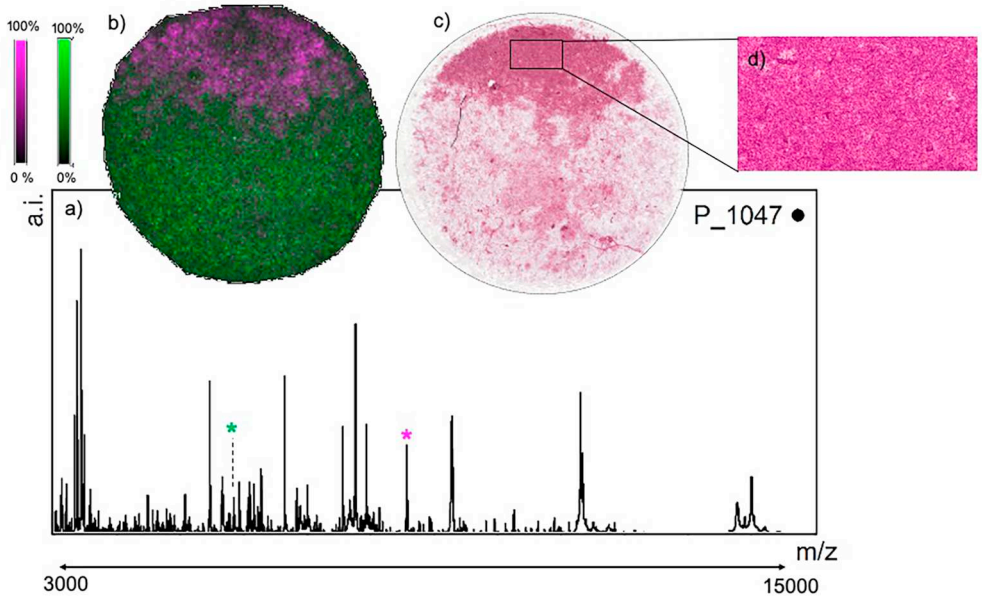

Fig. 3. a) Overall Average mass spectra from 3,000 to 15,000 *m/z*; b) MALDI-MSI Image of P_1047 with a signal (in pink) specifically localize in an area with an abundance of lymphocytes cells and a signal (in green) localize in an area with epithelial cells; c) Haematoxylin and Eosin Image; d) Zoom-in in the lymphocytes area.

Table 2
Classification probability (%) of being malignant, benign or Hashimoto thyrodite, for each patient of the validation set based on the average spectrum). In the Cytological Diagnosis column are reported details on the percentage of the different types of cells (Epithelial, Inflammatory background). Then for each patients the probability of being malignant, benign or Hashimoto thyroiditis looking at the average spectrum of the whole samples are reported.

Cytological Diagnosis	Patient ID	Classification Probability (%)		
		Hp	PTC	HT
THY2	1123	98,16	0,02	1,82
THY2	1156	89,80	0,12	9,99
THY2	278	99,97	0,00	0,03
THY2 (Hp=90% HT=10%)	316	85,60	0,07	14,25
THY2 (Hp=70% HT=30% with 10% oncocytes + Mϕ)	1075	95,43	4,50	0,07
THY2 (Hp=50% HT=50% with 10% oncocytes)	525	40,47	55,71	3,83
THY2 (Hp=50% HT=50%)	520	54,03	0,36	45,61
THY2 (Hp=20% HT=80%)	1234	34,32	0,49	65,19
THY2 (Hp=10% HT=90%)	1122	8,18	1,06	90,75
THY2 HT	1081	0,00	0,00	100,00
THY3 (Hp=90% HT=10%)	1082	87,30	3,91	8,79
THY4	1202	0,86	97,67	1,47
THY5	1084	100,00	0,00	0,00
THY5	1084 *ex-vivo*	7,56	92,21	0,23
THY5	1149	4,45	0,65	94,90
THY5	1188	97,23	1,57	1,20
THY5	1188 *ex-vivo*	1,18	98,70	0,11
THY5	11171 *ex-vivo*	9,42	87,53	3,06

Hp: Hyperplastic; HT: Hashimoto Thyroiditis; PTC: Papillary Thyroid Carcinoma; MΦ: macrophages.

exhibited higher glycosylation levels than those observed for TgAb IgG of healthy controls [30]. An earlier study by Wang demonstrated that the investigation of secreted cytokines such as interleukin-2 (IL-2) and IL-10 and interferon-γ by lymphocytes in HT might by contribute to the differentiation of different subsets of plasma cells, and subsequently affect the different levels of glycosylation on TgAb IgG [31]. Further studies will be required to investigate the role of cytokines in the thyroid tissue on TgAb glycosylation in greater detail. Our MALDI-MSI based approach clearly enlightens that HT should be included in the general scenario of benign nodules, adding to the hyperplastic features of goiter the proteomic components brought by the lymphocytic-rich background and (potentially) by the metaplastic (oxyphil) changes of the epithelium. The histograms of frequence of the training phase in Hp and HT (Supplementary Table 2) showed a low probability of being malignant (overall mean of the 3rd quartiles less than 7.5%; sd = 6.7), and a probability between an overall mean of the 1st and the 3rd quartiles of 20.9% and 64.7% respectively (sd = 27.0). However, specific discriminative signals characterize HT. The possibility to overlap the different ROIs of the H&E stained slides and the proteomic profile gave the opportunity to verify the specific weight of every single cellular component of the FNAs. This is particularly important since HT FNAs are challenging specimens in terms of heterogeneity with interspersed epithelial cells, macrophages and lymphocytes. A specific HT-linked group of signals was generated to separate HT patients from goiter (green) and malignant PTC (red). These signals (m/z) came from the average spectrum analysis of lymphocyte-rich areas on cytological slides. An additional advantage of the MALDI-MSI is to provide a correct classification using the pixel-by-pixel data avoiding the laborious and time consuming phase to define the ROIs by the pathologist. The existence of particular cases in the validation set characterized by some red signals of alert lays the foundations for the speculative hypothesis about the possible pathogenetic link between HT and cancer. In this contest, proteomics seems to confirm the existence of dysplastic/ borderline entities [8]. Although epidemiologic studies suggested an increased risk, the association between HT and PTC is still being debated [9]. Areas of cytologic atypia of the follicular epithelium in HT can be so prominent, to be mistaken for PTC. Chui et al. proposed the term *follicular epithelial dysplasia* for these atypical follicular epithelial proliferations with strong staining for HBME-1, galectin-3, CK19, and cyclin D1, supporting the concept of a premalignant lesion [32]. Genetic studies demonstrated a loss of heterozygosity in specific chromosomal regions, affecting tumor-suppressor genes in atypical foci of HT and *RET/PTC* rearrangements [33,34]. HT-profile may be identified for further pathogenetic investigations between HT and cancer. Finally, specific signal in FNAs may be translated into a tool for serum analysis as alternative diagnostic biomarkers in the future. Double (Tpo Ab-TgAb) negative patients may require the identification of new candidates, able to classify in the precision medicine era cases with hypothyroidism, ecographic suspicious of HT but absence of putative targets.

5. Conclusions

HT exhibits a complex etiology, which is currently incompletely understood. Thus, investigating the etiology of HT is paramount for the prevention and treatment of hypothyroidism. Proteomics may be

helpful not only in the diagnostic phase but also for prognostic implications, due to the possible pathogenetic link between HT and cancer. MALDI-imaging based approach enhanced statistically relevant HT-related peaks potentially usable in the future in the diagnostic workflow of HT.

Supplementary data to this article can be found online at https://doi.org/10.1016/j.bbapap.2020.140481.

Credit Author Statement

Giulia Capitoli: Methodology, Formal analysis, Software, Writing-Review & Editing.

Isabella Piga: Methodology, Investigation, Writing-Review & Editing.

Francesca Clerici: Methodology, Investigation, Writing-Review & Editing.

Virginia Brambilla: Investigation.

Allia Mahajneh: Investigation.

Davide Leni: Resources (Human samples, clinical data).

Mattia Garancini: Resources (Human samples, clinical data).

Angela Ida Pincelli: Resources (clinical data).

Vincenzo L'Imperio: Investigation.

Stefania Galimberti: Conceptualization, Supervision, Reviewing & Editing.

Fulvio Magni: Conceptualization, Supervision, Resources (Instrumentation, Reagents, Materials), Reviewing & Editing.

Fabio Pagni: Conceptualization, Resources (Human samples, clinical data), Funding acquisition and Project administration, Reviewing & Editing.

Declaration of Competing Interest

The authors declare that they have no known competing financial interests or personal relationships that could have appeared to influence the work reported in this paper.

Acknowledgments

This work was funded by AIRC (Associazione Italiana per la Ricerca sul Cancro) MFAG grant 2016- Id. 18445.

References

[1] M. Galli, I. Zoppis, G. De Sio, C. Chinello, F. Pagni, F. Magni, G. Mauri, A support vector machine classification of thyroid Bioptic specimens using MALDI-MSI data, Adv. Bioinforma. 2016 (2016) 3791214, https://doi.org/10.1155/2016/3791214.

[2] A. Smith, M. Galli, I. Piga, V. Denti, M. Stella, C. Chinello, N. Fusco, D. Leni, M. Manzoni, G. Roversi, M. Garancini, A.I. Pincelli, V. Cimino, G. Capitoli, F. Magni, F. Pagni, Molecular signatures of medullary thyroid carcinoma by matrix-assisted laser desorption/ionisation mass spectrometry imaging, J. Proteomics (2018), https://doi.org/10.1016/j.jprot.2018.03.021.

[3] Piga Isabella, Giulia Capitoli, Stefania Galimberti, Davide Leni, Angela Ida Pincelli, Mattia Garancini, Francesca Clerici, Allia Mahajneh, Virginia Brambilla, Andrew Smith, Fulvio Magni, Fabio Pagni, MALDI-MSI as a complementary diagnostic tool in cytopathology: a pilot study for the characterization of thyroid nodules, Cancers. 11 (2019) 1377, https://doi.org/10.3390/cancers11091377.

[4] R.M. Caprioli, Imaging mass spectrometry: molecular microscopy for enabling a new age of discovery: proteomics 2014, PROTEOMICS. 14 (2014) 807–809, https://doi.org/10.1002/pmic.201300571.

[5] M. Aichler, A. Walch, MALDI imaging mass spectrometry: current frontiers and perspectives in pathology research and practice, Lab. Investig. 95 (2015) 422–431, https://doi.org/10.1038/labinvest.2014.156.

[6] F. Pagni, G. De Sio, M. Garancini, M. Scardilli, C. Chinello, A.J. Smith, F. Bono, D. Leni, F. Magni, Proteomics in thyroid cytopathology: relevance of MALDI-imaging in distinguishing malignant from benign lesions, PROTEOMICS. 16 (2016) 1775–1784, https://doi.org/10.1002/pmic.201500448.

[7] F. Pagni, V. Mainini, M. Garancini, F. Bono, A. Vanzati, V. Giardini, M. Scardilli, P. Goffredo, A.J. Smith, M. Galli, G. De Sio, F. Magni, Proteomics for the diagnosis of thyroid lesions: preliminary report, Cytopathology. 26 (2015) 318–324, https://doi.org/10.1111/cyt.12166.

[8] J. Liang, W. Zeng, F. Fang, T. Yu, Y. Zhao, X. Fan, N. Guo, X. Gao, Clinical analysis of Hashimoto thyroiditis coexistent with papillary thyroid cancer in 1392 patients, Acta Otorhinolaryngol Ital. 37 (2017) 393–400, https://doi.org/10.14639/0392-100X-1709.

[9] R. Vita, A. Ieni, G. Tuccari, S. Benvenga, The increasing prevalence of chronic lymphocytic thyroiditis in papillary microcarcinoma, Rev. Endocrine and Metabolic Disorders. 19 (2018) 301–309, https://doi.org/10.1007/s11154-018-9474-z.

[10] G. Wu, Ultrasonography in diagnosis of Hashimoto rsquo s thyroiditis, Front. Biosci. 21 (2016) 1006–1012, https://doi.org/10.2741/4437.

[11] P. Caturegli, A. De Remigis, N.R. Rose, Hashimoto thyroiditis: clinical and diagnostic criteria, Autoimmun. Rev. 13 (2014) 391–397, https://doi.org/10.1016/j.autrev.2014.01.007.

[12] H. Guan, N.S. de Morais, J. Stuart, S. Ahmadi, E. Marqusee, M.I. Kim, E.K. Alexander, Discordance of serological and sonographic markers for Hashimoto's thyroiditis with gold standard histopathology, Eur. J. Endocrinol. 181 (2019) 539–544, https://doi.org/10.1530/EJE-19-0424.

[13] I. Piga, G. Capitoli, S. Tettamanti, V. Denti, A. Smith, C. Chinello, M. Stella, D. Leni, M. Garancini, S. Galimberti, F. Magni, F. Pagni, Feasibility study for the MALDI-MSI analysis of thyroid fine needle aspiration biopsies: evaluating the morphological and proteomic stability over time, PROTEOMICS – Clinical Applications. 13 (2019) 1700170, https://doi.org/10.1002/prca.201700170.

[14] I. Piga, G. Capitoli, V. Denti, S. Tettamanti, A. Smith, M. Stella, C. Chinello, D. Leni, M. Garancini, S. Galimberti, F. Magni, F. Pagni, The management of haemoglobin interference for the MALDI-MSI proteomics analysis of thyroid fine needle aspiration biopsies, Anal. Bioanal. Chem. 411 (2019) 5007–5012, https://doi.org/10.1007/s00216-019-01908-w.

[15] A. Pyzik, E. Grywalska, B. Matyjaszek-Matuszek, J. Roliński, Immune disorders in Hashimoto's thyroiditis: what do we know so far? J Immunol Res 2015 (2015) 1–8, https://doi.org/10.1155/2015/979167.

[16] M.I. Liontiris, E.E. Mazokopakis, A concise review of Hashimoto thyroiditis (HT) and the importance of iodine, selenium, vitamin D and gluten on the autoimmunity and dietary management of HT patients.Points that need more investigation, Hell J Nucl Med. 20 (2017) 51–56, https://doi.org/10.1967/s002449910507.

[17] Y. Hiromatsu, H. Satoh, N. Amino, Hashimoto's thyroiditis: history and future outlook, Hormones (Athens). 12 (2013) 12–18, https://doi.org/10.1007/BF03401282.

[18] G. Radetti, Clinical aspects of Hashimoto's thyroiditis, in: G. Szinnai (Ed.), Endocrine Development, S. KARGER AG, Basel, 2014, pp. 158–170, , https://doi.org/10.1159/000363162.

[19] R.A. Ajjan, A.P. Weetman, The pathogenesis of Hashimoto's thyroiditis: further developments in our understanding, Horm. Metab. Res. 47 (2015) 702–710, https://doi.org/10.1055/s-0035-1548832.

[20] E. Nishihara, N. Amino, T. Kudo, M. Ito, S. Fukata, M. Nishikawa, H. Nakamura, A. Miyauchi, Comparison of thyroglobulin and thyroid peroxidase antibodies measured by five different kits in autoimmune thyroid diseases, Endocr. J. 64 (2017) 955–961, https://doi.org/10.1507/endocrj.EJ17-0164.

[21] I. Ates, M.F. Arikan, M. Altay, F.M. Yilmaz, N. Yilmaz, D. Berker, S. Guler, The effect of oxidative stress on the progression of Hashimoto's thyroiditis, Arch. Physiol. Biochem. 124 (2018) 351–356, https://doi.org/10.1080/13813455.2017.1408660.

[22] D. Grimm, Cell and Molecular Biology of Thyroid Disorders, Int J Mol Sci. 20 (2019), https://doi.org/10.3390/ijms20122895.

[23] D. Lubin, E. Baraban, A. Lisby, S. Jalali-Farahani, P. Zhang, V. Livolsi, Papillary thyroid carcinoma emerging from Hashimoto thyroiditis demonstrates increased PD-L1 expression, which persists with metastasis, Endocr. Pathol. 29 (2018) 317–323, https://doi.org/10.1007/s12022-018-9540-9.

[24] H. Xiao, Y. Zhang, Y. Kim, S. Kim, J.J. Kim, K.M. Kim, J. Yoshizawa, L.-Y. Fan, C.-X. Cao, D.T.W. Wong, Differential Proteomic Analysis of Human Saliva using Tandem Mass Tags Quantification for Gastric Cancer Detection, Scientific Reports 6 (2016), https://doi.org/10.1038/srep22165.

[25] A. Cuomo, S. Moretti, S. Minucci, T. Bonaldi, SILAC-based proteomic analysis to dissect the "histone modification signature" of human breast cancer cells, Amino Acids 41 (2011) 387–399, https://doi.org/10.1007/s00726-010-0668-2.

[26] M. Stella, C. Chinello, A. Cazzaniga, A. Smith, M. Galli, I. Piga, A. Grasso, M. Grasso, M. Del Puppo, M. Varallo, G. Bovo, F. Magni, Histology-guided proteomic analysis to investigate the molecular profiles of clear cell renal cell carcinoma grades, J. Proteome 191 (2019) 38–47, https://doi.org/10.1016/j.jprot.2018.04.028.

[27] F. Ciregia, C. Giacomelli, L. Giusti, C. Boldrini, I. Piga, P. Pepe, A. Consensi, S. Gori, A. Lucacchini, M.R. Mazzoni, L. Bazzichi, Putative salivary biomarkers useful to differentiate patients with fibromyalgia, J. Proteome 190 (2019) 44–54, https://doi.org/10.1016/j.jprot.2018.04.012.

[28] A.A. Alfadda, H. Benabdelkamel, A. Masood, A.A. Jammah, A.A. Ekhzaimy, Differences in the Plasma Proteome of Patients with Hypothyroidism before and after Thyroid Hormone Replacement: A Proteomic Analysis, Int J Mol Sci. 19 (2018), https://doi.org/10.3390/ijms19010088.

[29] Y. Hirao, S. Saito, H. Fujinaka, S. Miyazaki, B. Xu, A.F. Quadery, A. Elguoshy, K. Yamamoto, T. Yamamoto, Proteome Profiling of Diabetic Mellitus Patient Urine for Discovery of Biomarkers by Comprehensive MS-Based Proteomics, Proteomes 6 (2018), https://doi.org/10.3390/proteomes6010009.

[30] S. Yuan, Q. Li, Y. Zhang, C. Huang, H. Wu, Y. Li, Y. Liu, N. Yu, H. Zhang, G. Lu, Y. Gao, Y. Gao, X. Guo, Changes in anti-thyroglobulin IgG glycosylation patterns in Hashimoto's thyroiditis patients, J. Clin. Endocrinol. Metab. 100 (2015) 717–724, https://doi.org/10.1210/jc.2014-2921.

[31] J. Wang, C.I.A. Balog, K. Stavenhagen, C.A.M. Koeleman, H.U. Scherer,

M.H.J. Selman, A.M. Deelder, T.W.J. Huizinga, R.E.M. Toes, M. Wuhrer, Fc-glycosylation of IgG1 is modulated by B-cell stimuli, Mol. Cell. Proteomics 10 (2011), https://doi.org/10.1074/mcp.M110.004655 (M110.004655).

[32] M.H. Chui, C.A. Cassol, S.L. Asa, O. Mete, Follicular epithelial dysplasia of the thyroid: morphological and immunohistochemical characterization of a putative preneoplastic lesion to papillary thyroid carcinoma in chronic lymphocytic thyroiditis, Virchows Arch. 462 (2013) 557–563, https://doi.org/10.1007/s00428-013-1397-1.

[33] F. Matsumoto, H. Fujii, M. Abe, K. Kajino, T. Kobayashi, T. Matsumoto, K. Ikeda, O. Hino, A novel tumor marker, Niban, is expressed in subsets of thyroid tumors and Hashimoto's thyroiditis, Hum. Pathol. 37 (2006) 1592–1600, https://doi.org/10.1016/j.humpath.2006.06.022.

[34] F. Ragusa, P. Fallahi, G. Elia, D. Gonnella, S.R. Paparo, C. Giusti, L.P. Churilov, S.M. Ferrari, A. Antonelli, Hashimotos' thyroiditis: epidemiology, pathogenesis, clinic and therapy, Best Pract. Res. Clin. Endocrinol. Metab. 33 (2019) 101367, https://doi.org/10.1016/j.beem.2019.101367.